International Journal of Thin Films Science and Technology

http://dx.doi.org/10.18576/ijtfst/110302

Structure of the Deformed 7075 Aircraft Al - Alloy with Material Analysis Using Diffraction (MAUD)

Z. Sayed[1], M. Abdel-Rahman[1], M. Y. A Mostafa[1,2], M. A. Abdel-Rahman[1], E. A. Badawi[1,*], E. E. Assem[3] and A. Ashour[1,3]

[1]Physics Department, Faculty of Science, Minia University, 61519, Egypt
[2]Experimental Physics Department, Physics and Technology Institute, Ural Federal University, Ekaterinburg, Russia, 620002
[3]Physics Department, Faculty of Science, Islamic University, Kingdom of Saudi Arabia

Received: 18 May. 2022, Revised: 5 Jul. 2022, Accepted: 23 Jul. 2022.
Published online: 1 Sep. 2022.

Abstract: This work aims to study the effect of plastic deformation on the 7075 Al - alloy using Material Analyses Using Diffraction (MAUD). Plastic deformation produces dislocation defects. Using a hydraulic press, samples were deformed up to 25%. The XRD was measured for each degree of deformation. The MAUD program was used to analyze the data, and mathematical methods were deployed to understand the various behaviors observed. The lattice parameter, crystallite size, average internal stress, micro-strain, and dislocation density of the 7075Al-alloy were calculated. As the deformation degree increased, there was a progressive decline in the crystallite size as an increase in the micro-strain and dislocation density. The flow stress changes from 5.8 to 49 MPa and the stored dislocation energy varies from 2.62 to 185 kPa.

Keywords: 7075 Al – alloy, MAUD, plastic deformation, XRD.

1 Introduction

Aluminum alloys have been extensively applied in the construction industries, automotive, and aircraft on account of their coveted physical and substantial properties. Due to their perfect strength-to-weight ratio and resistance to stress corrosion, high-strength Al-Zn-Mg-Cu alloys (like the 7075 Al alloy) are extremely utilized in the aeronautics, marine, and automotive industries [1, 2]. The aluminum alloys series 7xxx is considered one of the most useful engineering materials [3]. Such alloys have highly desirable physical and mechanical properties, such as elevated strength and corrosion engaging behavior in several media [1, 2, 4].

Several kinds of crystalline defects have a significant enhancement effect on the materials property, including point defects, vacancies, and dislocation line. Alloy composition and heat treatments are used on 7000-series aluminum alloys to attain a perfect adjustment between strength force and deterioration toleration [5]. The various behaviors of Al-Zn-Mg-Cu alloys with deformation have been studied to demonstrate the operation of deformation mechanisms during hardening work [6, 7], re-crystallization (DRX) [8, 9] and dynamic recovery (DRV) [10, 11]. The workability of material can be enhanced through grasping the metal flow behavior. The 7000-series aluminum alloys are used in a diverse range of engineering projects, as their mechanical properties can be improved and modified by means of heat handling treatment or processing of thermo-mechanical [12 – 14]. The aluminum alloy 7075 is considered one of the strongest aluminum alloys [15] because it makes the material fit for application, such as aircraft parts or parts subject to heavy wear [16]. This alloy has a high yield strength of more than 500 MPa, while with low density, this alloy is suitable to use in aircraft accessories. Also, it has less resistant corrosion compared to other alloys, its strength makes up for this disadvantage [15].

Plastic deformation is a perpetual shape alteration and it is irreversible deformation. This deformation appears in alloys or metals when they are affected by loads that exceed the required energy to fetch dislocations [17, 18]. The structural materials election encompasses compromising between strength and ductility since materials with high ductility normally have low strength and vice versa [19 – 22]. Ordinarily, FCC metals display the ductility higher and BCC metals display the strength higher. For structural materials,

*Corresponding author E-mail: emad.badawi@mu.edu.eg

the most eligible feature is to turn stronger when deformed with cold work until it reaches an assured deformation degree. The expended energy on the plastic deformation of alloy or metal is fundamentally divided into two parts: the first one is converted for heat depending on the loading and degree of deformation types, while the second is stored into the defects as a strain energy form [18]. At this case, the alloy turns into an energy battery. The stored energy over cold work has been specified and described experimentally by numerous studies [2, 12,13, 15, 17, 19, 22 – 24].

X-ray diffraction (XRD) is a powerful nondestructive technique for characterizing crystalline materials. It provides information on structures, phases, preferred crystal orientations (texture), and other structural parameters, such as average grain size, crystallinity, strain, and crystal defects. X-ray diffraction peaks are produced by constructive interference of a monochromatic beam of X-rays scattered at specific angles from each set of lattice planes in a sample. The peak intensities are determined by the distribution of atoms within the lattice [21].

The present work aims to study the plastic deformation effect (thickness reduction) on the structure of 7075-aluminum alloy (defect density, dislocation density, flow stress analysis and stored dislocation energy) with X-ray diffraction techniques. Plastic deformation with a thickness reduction up to 25% was applied using a hydraulic press. As mentioned in literature, the electrical conductivity didn't change significantly, while the micro-hardness for 7075 Al alloy extremely improved with deformation.

2. Experimental work

2.1. Sample preparation

The 7075 Al alloy chemical *installation* is presented in **Table 1.** The samples were cut into squares measuring 13×13×3 mm^3. The surfaces of the samples were grounded with silica carbide papers of various sizes. After grinding, the specimens were polished for 5 minutes in a mixed solution of nitric acid and phosphoric acid to obtain a bright surface and remove any scratches or surface dust created during the preparation process. Then, the specimens were annealed at 773 Kelvin for 6 hours and cooled to room temperature to provide samples without any thermal stresses.

Table 1: The 7075 Al alloy chemical installation.

Element	Weight%
Cr	0.23
Cu	1.60
Mg	2.50
Zn	5.60
Al	remint

The deformation is applied on the annealed samples at RT up to 25% from the original thickness utilizing a hydraulic press (applied external work) to obtain different degrees of deformation (thickness reductions). The degree of deformation is expressed as a thickness proportion according to:

$$\textbf{Deformation (\%)} = \frac{\Delta D}{D_0} = \frac{D_0 - D}{D_0} \quad (1)$$

where D and D_0 are the thickness after deformation and the initial thickness respectively.

2.2. X-ray diffraction technique

Measurements with XRD were achieved utilizing an A JEOL X-ray (JSDX-60PA) diffractometer with an attached Ni-filtered Cu-Kα radiation source (λ = 0.154184 nm). The source of X-ray was operated at 40 kV and 35 mA. A 2θ range from 35° to 85° was scanned at a continuous slow scanning rate (1° / min) and a low constant time (1 sec) to find the required diffraction peaks. XRD measurements were accomplished for the identification of phase and the preferred orientation statement. The preferred orientation can be distinguished between the original (0% d before deformation) and the end of deformation as presented. It is meaning the change of the arbitrary units of the intensity. In some recent studies, MAUD has been applied to determine materials parameters of the micro structural, including cell parameter, crystallite size (D) and residual micro-strain (ε). Detailed methods of the micro structural test have been stated in recently published reports [25 – 32].

***Dislocation density* (ρ):**

The dislocation density (ρ, cm^{-2}) can be calculated by using the following equation [33]:

$$\rho \quad (\mathbf{cm^{-2}}) \quad = \quad \frac{3\sqrt{2\pi}\sqrt{\varepsilon^2}}{D\,b} \quad (2)$$

where D is the crystallite size average and ε is the micro-strain, b is the Burgers vector (for Al alloys, $b = a/\sqrt{2} = 2.86$ Å) at the FCC structure and a is the lattice parameter.

***Defect Density* (ρ^-):**

The defect density (ρ^-, cm^{-3}) is calculated from the dislocation density (expressed as length per unit volume) with the following equation [34]:

$$\rho^-(cm^{-3}) = \frac{\rho(cm^{-2})}{b} \quad (3)$$

***Flow stress* (τ):**

The flow stress is expressed in terms of τ (the resolved shear stress) relatives to the root square of the dislocation density. It is calculated by the following equation [34]:

$$\tau = \tau_0 + \alpha\, G\, b\, \sqrt{\rho} \quad (4)$$

where τ_0 is the friction stress, α is the dislocation interaction parameter (constant with order of 0.5) and the dislocation

interaction parameter, G is the shear modulus and b is Burgers vector**.** In terms of tensile stress, by taking the friction stress as equal to zero and $\sigma = M\,\tau$, the flow stress (σ) is calculated via the following equation [32]**:**

$$\sigma = M\,\alpha\,G\,b\,\sqrt{\rho} \qquad (5)$$

where M is the Taylor factor average and G is the shear modulus of Al-alloy = 26 GPa**.** The above relationship is then given by**:**

$$\tau = \alpha\,G\,b\,\sqrt{\rho} \qquad (6)$$

Dislocation Stored Energy **(E):**

There is a dependent relationship between the stored energy and plastic deformation (the cold work amount) that gained via the material [35]**.** The alloy that deformed with plastic deformation mainly contains a major amount of dislocation stored energy**:** at higher temperatures with annealing and during recovery or recrystallization, the alloy will typically restore to a minimum state of energy through the growth of structural [36]**.** The dislocation stored energy (E), caused by the obstetrics of the crystal defects can be specified on the dislocation theory basis**.** The dislocation density (ρ) is regarding the dislocation stored energy as the following Eq**.** [36]**.**

$$E = \alpha\,\rho\,G\,b^2 \qquad (7)$$

XRD provides an indirect way to determine the dislocation of stored energy in the case of plastic deformation (cold work is applied)**.** In such case, the stored dislocation energy can be calculated by substituting the dislocation density values from equations 2 to 6**.**

3. Results and discussions

X-ray diffraction of the non-deformed and deformed 7075 Al alloy samples with various plastic deformation degrees from 0 to 24**.**9% are presented in **Fig. 1.** The main diffraction patterns feature nearly the same, although the peak intensity is varied from one sample to another**.** Also, there are no peaks for the free Mg was observed**.** The observed peaks of diffraction are founded at 2θ = 38**.**5, 44**.**8, 65**.**2, 78**.**1 and 82**.**30 correspond to the planes (111), (200), (220), (311) and (222), respectively [37, 38]**.** However, in all samples, the planes (111) and (200) intensities were quite high compare with the other planes of diffraction**.** This indicates to planes that are the discriminatory preferred orientation of the microcrystalline structure**.** The preferred orientation distinguishing is between the original (0% d before deformation) and the end of deformation as presented (24**.**9% d)**.** In such case, the change of the arbitrary units of the intensity especially for the first two strong peaks**.** The XRD spectra were analyzed with MAUD**.** Then the parameters (grain size, micro-strain, lattice parameter, and d-spacing) were obtained**.**

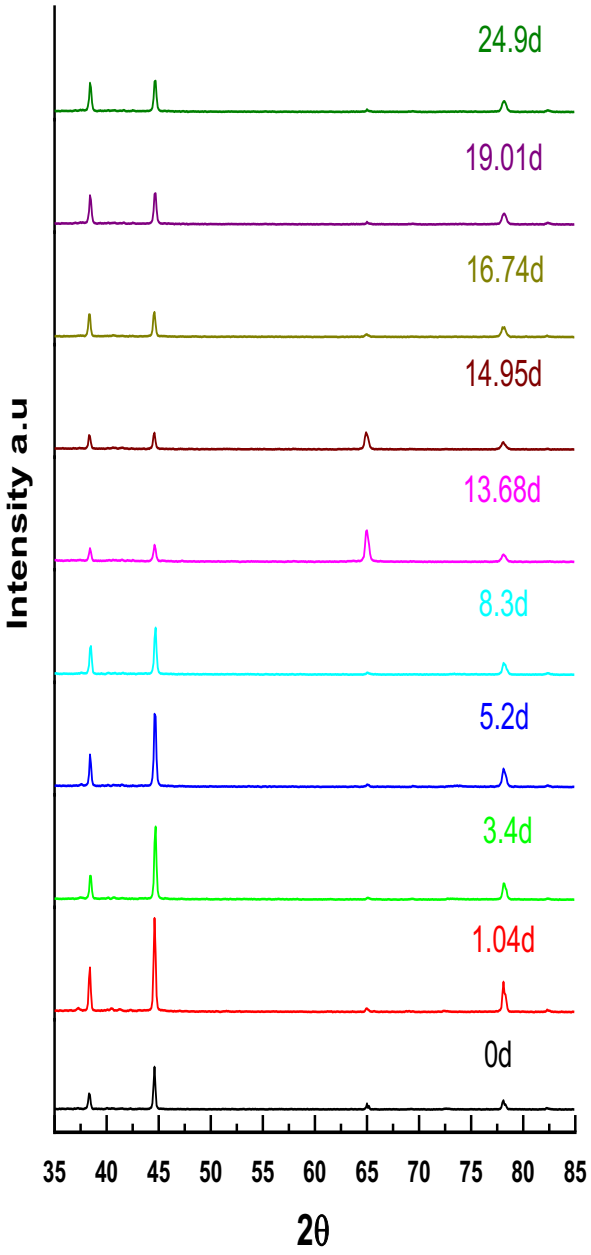

Fig. 1: X-ray diffracto-grams of Al alloy the 7075 depending on the deformation degree.

3.1. Microstructure analysis with Riveted refinement (MAUD program)

The initial microstructure of 7075 Al alloy is shown in **Table 2**, which before deformation processing the crystallite size had high value, is about as 1**.**237 µm, the micro-strain had low value 1**.**16 x 10^{-4} and the cell parameter for most thickness reduction varies around 4**.**00 Å**.** The refined parameters obtained from X-ray analysis (micro-strain cell, crystallite and cell parameter) are presented in figures 2, 3 and 4**.** The cell parameter is nearly constant with the deformation of the 7075 Al alloy up to 25%**.** The

behavior of the cell parameter depending on the thickness reduction is explained in **Fig. 2**, revealing a cell parameter value of around 4.00 Å**.** The change in lattice constant for the deformed 7075 Al-alloy indicates that the deformed grains are strained**.**

The crystallite size depending on the thickness reduction is explained in **Fig. 3** with exponential fitting**.** It is clear that crystallite size decreases exponentially as thickness reduction from 1.237 µm (for a non-deformed sample) to 0.205 µm (24.9% thickness reduction)**.** This decrease supposedly interpreted in terms of columnar grain growth**.** In contrast, the micro-strain revealed a different behavior, the micro-strain increases exponentially as thickness reduction increases**.** For a non-deformed sample, the micro-strain is 1.16 x 10^{-4}**:** this reaches 10.7 x 10^{-4} at 16.74% deformation**.** This variation may be due to the increase of the structural defects among which the grain boundary**.** The behavior of micro-strain depending on the thickness reduction is explained in **Fig. 4** with exponential fitting**.**

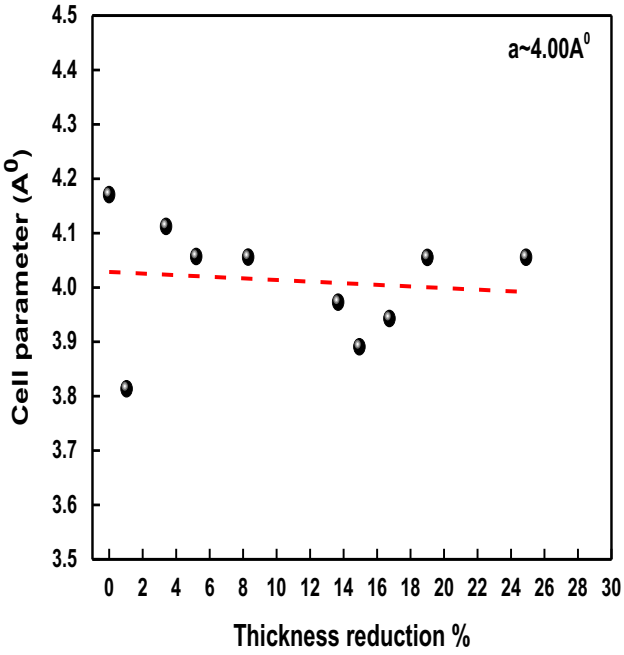

Fig. 2: The lattice parameter depending on the 7075 Al alloy deformation.

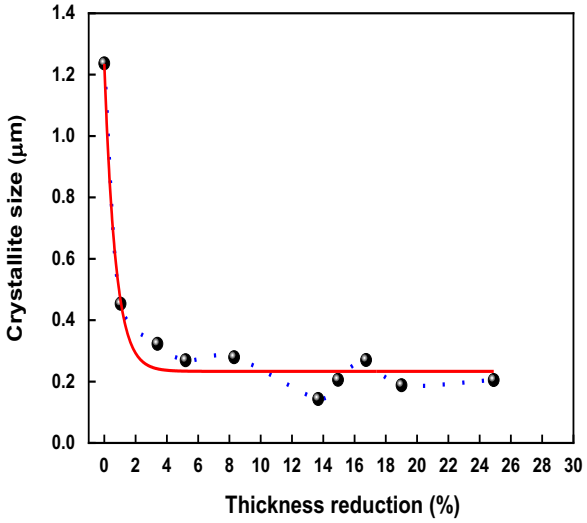

Fig. 3: Variation of crystallite size with the deformation of the 7075 Al alloy.

The variation of d_{hkl} as a function of 2θ is shown in **Fig. 5.** The d-spacing values for the five (hkl) planes decrease as a function of 2θ at various thicknesses reduction levels**.** There is also no change is observed in the d-spacing for different levels of thickness reduction**.** A comparison of observed and standard d-spacing values (hkl) planes as matched indicates that the tested samples from 7075 Al-alloy are polycrystalline with a face-centered cubic structure**.** The peak intensities increase probably accredited to growth grain connected with the increase in the crystalline degree by raising the percentage of deformation**.**

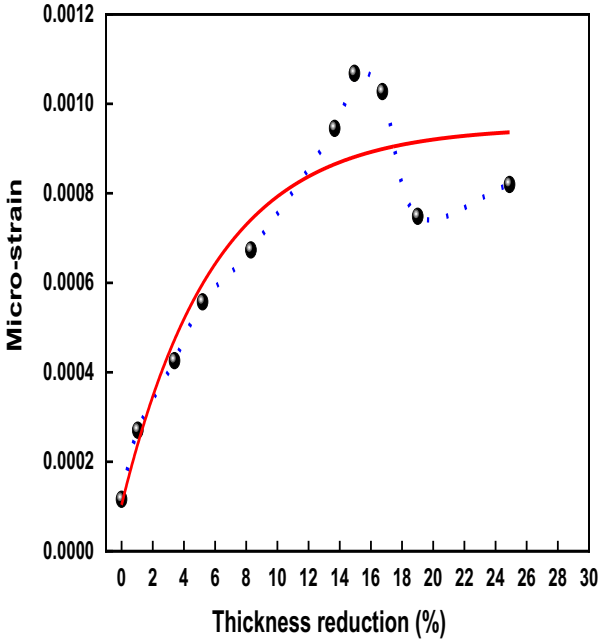

Fig. 4: Variation of micro-strain with the deformation of the 7075 Al alloy.

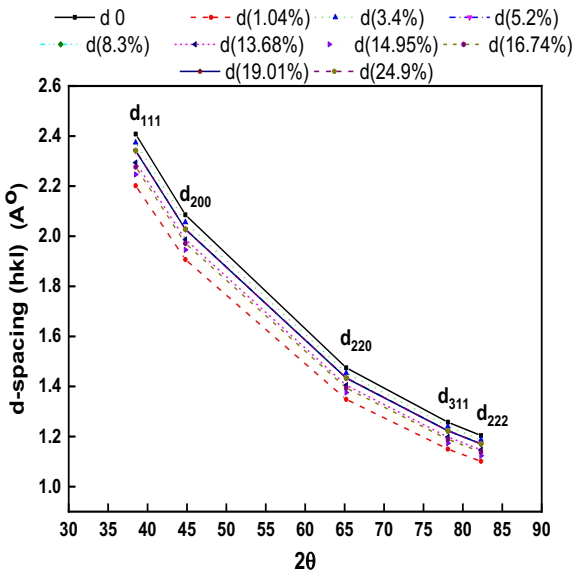

Fig. 5: D_{hkl} depending on 2θ for the Al alloy 7075 at various deformation levels.

3.2. Dislocation and defect density, flow stress and stored energy

The results of dislocation and defect densities, flow stress and stored energy applying the X-ray diffraction analysis are presented in **Table 2.**

The crystallite size average values and micro-strain present the dislocation density of samples at various levels of true strain (**ε**)**:** these values are listed in **Table 2.** As clear, as the applied stress increases the micro-strain also increases**.** The decline in the crystallite size is not noteworthy**.** The restricted extent of the macroscopic strain that applied through the tensile test compared to the plastic deformation techniques probably accountable for the crystallite size trivial changes [39, 40]**.** In the present work, although the average calculated crystallite size is comparatively small but has a strong effect on the dislocation density**.**

The dislocation and defect densities reveal the same behavior as the 7075 Al alloy's micro-strain**.** It is clear from these two figures that the dislocation and defect densities increase exponentially as the degree of deformation increases**.** Maximum values of the dislocation and defect densities of about 1.73 x 10^{10} cm^{-2} and 6.04 x 10^{17} cm^{-3}, respectively, are obtained at approximately 13.68% deformation**.**

In the same way, the flow stress behavior depending on the thickness reduction increases exponentially from 5.8 MPa for a non-deformed sample to about 49.0 MPa at 13.68% deformation (**Fig. 6**)**.** From **Fig. 4** and **6** we can observe a good correlation for preferred orientation with the flow stress and micro strain**.**

Table 2: The dislocation density, defect density, flow stress and stored energy obtained from analysis of the X-ray diffraction data with MAUD for the Al alloy 7075 at various degrees of deformation.

Thickness reduction %	Dislocating density (cm^{-2})	Defect density (cm^{-3})	Flow stress (MPa)	Stored energy (kPa)
0	2.46E+08	8.61E+15	5.8	2.62
1.04	1.57E+09	5.48E+16	14.7	16.7
3.4	3.47E+09	1.21E+17	22	36.9
5.2	5.43E+09	1.90E+17	27.4	57.8
8.3	6.34E+09	2.22E+17	29.6	67.4
13.68	1.74E+10	6.07E+17	49.0	185
14.95	1.36E+10	4.77E+17	43.4	145
16.74	1.00E+10	3.50E+17	37.2	106
19.01	1.05E+10	3.66E+17	38.1	111
24.9	1.05E+10	3.68E+17	39.35	112

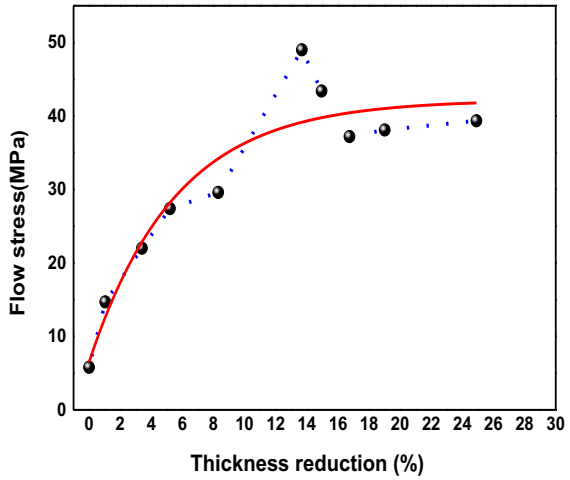

Fig. 6: The flow stress of the Al alloy 7075 depending on thickness reduction.

The minimum dislocation stored energy is 2.62 KPa at 0% deformation**.** Then the dislocation stored energy slowly increases at low thickness reduction levels**.** The dislocations prospect is small at low deformation levels**.** As the degree of deformation increases, the dislocations probability grows leading to an excess in the calculated stored dislocation energy**.** This action is due to a faster increase of E at high thickness reduction levels**.** The dislocation stored energy reaches a maximum (~185 KPa) at 13.68% deformation**.**

As mentioned in the literature to study the crystallite size growth against deformation (cold rolling) level for 7075 Al alloys [41 – 43], a universal decrease of the coherent domain size with the deformation level**.** The more a metallic material

deforms, the more the size of the coherent domain's decreases [41]. The variations in the crystallite size results from alloying elements, which are known to inhibit the growth of grain. In the case of grain refinement below 1 μm, the electrical conductivity didn't change significantly while the micro-hardness for 7075 Al alloy extremely improved [42]. The micro-strain in this alloy slightly increases with the deformation level. In addition, there is a synoptic increase in the dislocation density with the level of deformation [41].

The variation of flow stress with micro-strain is shown in **Fig. 7.** The strain effects on the various materials properties have been investigated elsewhere [6, 44 – 46]. The ductility increase of the Al alloy 7075 had been reported by Magd and Abouridouane [44]. Metallographic fulfillments for materials ductile (plastic) shear failure. Lee et al [6] estimated that for Al alloy 7075, two sensitive regions of strain rate appear through the strain rates range.

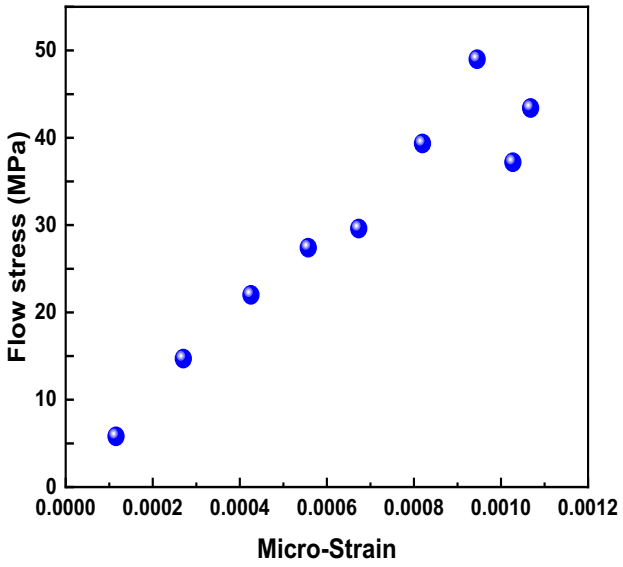

Fig. 7: Flow stress with micro-strain for the deformed 7075 Al alloy.

4. Conclusion

- The degree of preferred orientation was found to play a dominant role in the alloy's micro structural parameters. The optimum crystallization was observed at a deformation of 13.68%. At higher levels of thickness reduction (24.9%), crystal agglomeration often decomposed.
- The lattice constant, internal stress, crystallite size, micro-strain and dislocation density were estimated. At higher levels of deformation, crystallite size progressively declines while the dislocation density and micro-strain increase.

The flow stress changes from 5.8 to 49 MPa. The stored dislocation energy varies from (2.62 to 185) KPa. The flow stress variation with the micro-strain is clear and reflects changes in other structural properties.

References

[1] Jenab A and Taheri A K. Evaluation of low strain rate constitutive equation of 7075 aluminium alloy at high temperature *Materials Science and Technology* **27** 1067–72. 2011

[2] Obiko J and Mwema F. Deformation behaviour of high-strength aluminium alloy during forging process using finite element method *Engineering Solid Mechanics* **9** 31–40. 2020

[3] Guo Y, Zhou M, Sun X, Qian L, Li L, Xie Y, Liu Z, Wu D, Yang L, Wu T, Zhao D, Wang J and Zhao H . Effects of temperature and strain rate on the fracture behaviors of an Al-Zn-Mg-Cu alloy *Materials* **11** 1–15. 2018

[4] Lianggang G, Shuang Y, He Y and Jun Z 2015 Processing map of as-cast 7075 aluminum alloy for hot working *CHINESE JOURNAL OF AERONAUTICS* 1–10.

[5] Reed-Hill R A L A R E . *Metallurgy Physical Principles*. 2009

[6] Lee W-S, Sue W-C L, Wu C-F and Chin-Jyi. The strain rate and temperature dependence of the dynamic impact properties of 7075 aluminum alloy *Journal of Materials Processing Technology* **100** 116–22. 2000

[7] Shin D H, Lee C S and Kim W J . Superplasticity of fine-grained 7475 Al alloy and a proposed new deformation mechanism Acta Materialia **45** 5195–202. 1997

[8] Voyiadjis G Z and Abed F H. Microstructural based models for bcc and fcc metals with temperature and strain rate dependency *Mechanics of Materials* **37** 355–378. 2005

[9] Wang L, Yu H, Lee Y and Kim H W . Hot tensile deformation behavior of twin roll casted 7075 aluminum alloy *Metals and Materials International* **21** 832–41. 2015

[10] Srivatsan T S, Guruprasad G and Vasudevan V K. The quasi static deformation and fracture behavior of aluminum alloy 7150 *Materials and Design* **29** 742–51. 2008

[11] Picu R C, Vincze G, Ozturk F, Gracio J J, Barlat F and Maniatty A M. Strain rate sensitivity of the commercial aluminum alloy AA5182-O *Materials Science and Engineering A* **390** 334–43. 2005

[12] Li X and Starink M J. Effect of compositional variations on characteristics of coarse intermetallic particles in overaged 7000 aluminium alloys

Materials Science and Technology **17** 1324–8**.** 2001

[13] Dx T X S. International Journal of Impact Engineering Study of the constitutive behavior of 7075-T651 aluminum alloy Chandel D6X b Gupta c *International Journal of Impact Engineering* **108** 171–90**.** 2017

[14] Sajadifar S V, Scharifi E, Weidig U, Steinhoff K and Niendorf T. Performance of thermo-mechanically processed AA7075 alloy at elevated temperatures—from microstructure to mechanical properties *Metals* **10** 1–14**.** 2020

[15] Taheri-Mandarjani M, Zarei-Hanzaki A and Abedi H R. Hot ductility behavior of an extruded 7075 aluminum alloy *Materials Science and Engineering A* **637** 107–22**.** 2015

[16] Berlanga-Labari C, Biezma-Moraleda M V. and Rivero P J. Corrosion of cast aluminum alloys: A review *Metals* **10** 1–30**.** 2020

[17] Mittemeijer E J. Mechanical Strength of Materials *Fundamentals ofMaterials Science,* (Springer-Verlag Berlin Heidelberg 2010) pp 497–581**.** 2010

[18] Megson T H G. *Aircraft Structures* (AMSTERDAM • BOSTON • HEIDELBERG • LONDON • NEW YORK • OXFORD PARIS • SAN DIEGO • SAN FRANCISCO • SINGAPORE • SYDNEY • TOKYO**:** Butterworth-Heinemann is an imprint of Elsevier)**.** 2007

[19] Arora H S, Ayyagari A, Saini J, Selvam K, Riyadh S, Pole M and Grewal H S. High Tensile Ductility and Strength in Dual-phase Bimodal Steel through Stationary Friction Stir Processing *Scientific Reports* 1–6**.** 2019

[20] Liu Z Q and Z F Z. Mechanical properties of structural amorphous steels**:** Intrinsic correlations, conflicts, and optimizing strategies *J.Appl.Phys* **114243519** 1–14**.** 2013

[21] Abd-Elhakim M H, Mostafa M, Darwash M, Abdel-Rahman M, Abdel-Rahman M A and Badawi E A. Probing properties of 6061 aluminum alloy used as cladding for nuclear reactor fuel with X-ray diffraction *AIP Conference Proceedings* **2313.** 2020

[22] Ashby M F. *MATERIALS SELECTION SECOND EDITION MECHANICAL DESIGN* ed M F Ashby (OXFORD AUCKLAND BOSTON JOHANNESBURG MELBOURNE NEWDELHI**:** Butterworth-Heinemann)**.** 1999

[23] Abdel-Rahman M. Determination of the Positron Parameters and the Stored Dislocation Energy of Plastically Deformed Wrought 3004 Al- Alloy *Int. J. New. Hor. Phys.* **47** 43–7**.** 2017

[24] Feng A H, Chen D L and Ma Z Y. Microstructure and Cyclic Deformation Behavior of a Friction-Stir-Welded 7075 Al Alloy *METALLURGICAL AND MATERIALS TRANSACTIONS A* **41** 957–71**.** 2010

[25] Sahu P, Hamada A S, Ghosh R N, Karjalainen L P, X-ray Diffraction Study on Cooling-Rate-Induced γ fcc → ε hcp Martensitic Transformation in Cast-Homogenized Fe26Mn0**.**14C Austenitic Steel *METALLURGICAL AND MATERIALS TRANSACTIONS, September 2007 A* **38A**(9): 1991-2000

[26] Filho I R S, Sandim M J R, Ponge D, Sandim H R Z and Raabe D. Strain hardening mechanisms during cold rolling of a high-Mn steel**:** Interplay between submicron defects and microtexture *Materials Science & Engineering A* **754** 636–49**.** 2019

[27] Sahu P and De M. Microstructural characterization of Fe – Mn – C martensites athermally transformed at low temperature by Rietveld method *Materials Science and Engineering* **333** 10–23**.** 2002

[28] Sahu P and Kajiwara S. M icrostructural characterization of stress-induced martensites evolved at low temperature in deformed powders of Fe–Mn–C alloys by the Rietveld method *Journal of Alloys and Compounds* **346** 158–69**.** 2002

[29] Pal H and Chanda A. Characterisation of microstructure of isothermal martensite in Fe–23 Ni – 3**.**8 Mn by Rietveld method *Journal of Alloys and Compounds* **278** 209–15**.** 1998

[30] Zhan K, Fang W Q, Zhao B, Yan Y, Feng Q and Jiang C H. INVESTIGATION OF SURFACE GRADIENT MICROSTRUCTURE OF SHOT PEENED S30432 STEEL BY X-RAY LINE PROFILE ANALYSIS METHOD *Surface Review and Letters* **24** 1–6**.** 2017

[31] Chanda A. X-ray characterization of the microstructure of a -CuTi alloys by Rietveld's method *Journal of Alloys and Compounds 313* **313** 104–14**.** 2000

[32] Dini G, Ueji R, Najafizadeh A and Monir-vaghefi S M. Flow stress analysis of TWIP steel via the XRD measurement of dislocation density *Materials Science & Engineering A* **527** 2759–63**.** 2010

[33] Smallman R E and Westmacott K H. Stacking faults in face-centred cubic metals and alloys *Philosophical Magazine ISSN:* **2** 669–83**.** 1957

[34] Polycrystals F C C C-W and Rosen M. Annihilation of Positrons in F.C.C. Cold- Worked Polycrystals *J. BARAM and M. ROSE* **16** 263–72**.** 1973

[35] Titchener A L and Bever M. BTHE STORED ENERGY OF COLD WORK *PROGRESS In METAL PHYSICS* pp 247–338**.** 1958

[36] Baker I, Louis L L L and Mandal D. THE EFFECT OF GRAIN SIZE ON THE STORED ENERGY OF COLD WORK AS A FUNCTION OF STRAIN FOR POLYCRYSTALLINE NICKEL *Seripta MetatJurgiea ef Materialia* **32** 167–71**.** 1995

[37] Taheri-Mandarjani M, Zarei-Hanzaki A and Abedi H R. Hot ductility behavior of an extruded 7075 aluminum alloy *Materials Science and Engineering A* **637** 107–22**.** 2015

[38] Zhao Y H, Liao X Z, Jin Z, Valiev R Z and Zhu Y T. Microstructures and mechanical properties of ultrafine grained 7075 Al alloy processed by ECAP and their evolutions during annealing *Acta Materialia* **52** 4589–99**.** 2004

[39] Gubicza J, Chinh N Q, Lábár J L, Dobatkin S, Us Z H and Langdon T G. Correlation between microstructure and mechanical properties of severely deformed metals *Journal of Alloys and Compounds* **483** 271–4**.** 2009

[40] Gubicza J, Chinh N Q, Horita Z and Langdon T G. Effect of Mg addition on microstructure and mechanical properties of aluminum *Materials Science and Engineering A* **387**–**389** 55–9**.** 2004

[41] Lipińska M, Bazarnik P and Lewandowska M. The influence of severe plastic deformation processes on electrical conductivity of commercially pure aluminium and 5483 aluminium alloy *Archives of Civil and Mechanical Engineering* **16** 717–23**.** 2016

[42] Khereddine A, Hadj-Larbi F, Djebala L, Azzeddine H, Alili B and Bradai D. X-ray diffraction analysis of cold-worked Cu-Ni-Si and Cu-Ni-Si-Cr alloys by Rietveld method *Transactions of Nonferrous Metals Society of China (English Edition)* **21** 482–7**.** 2011

[43] Hamu G Ben, Eliezer D and Wagner L. The relation between severe plastic deformation microstructure and corrosion behavior of AZ31 magnesium alloy *Journal of Alloys and Compounds* **468** 222–9**.** 2009

[44] El-Magd E and Abouridouane M. Characterization , modelling and simulation of deformation and fracture behaviour of the light-weight wrought alloys under high strain rate loading *International Journal of Impact Engineering* **32** 741–58**.** 2006

[45] Puchi-cabrera E S, Staia M H, Ochoa-pérez E and Barbera-sosa J G La. Flow stress and ductility of AA7075-T6 aluminum alloy at low deformation temperatures *Materials Science & Engineering A* **528** 895–905**.** 2011

[46] Bobbili R, Ramakrishna B, Madhu V and Gogia A K. ScienceDirect Prediction of flow stress of 7017 aluminium alloy under high strain rate compression at elevated temperatures *Defence Technology* **11** 93–8**.** 2015